HHS Public Access

Author manuscript

Biol Psychiatry Cogn Neurosci Neuroimaging. Author manuscript; available in PMC 2017 November 01.

Published in final edited form as:

Biol Psychiatry Cogn Neurosci Neuroimaging. 2016 November ; 1(6): 528–538. doi:10.1016/j.bpsc.2016.08.007.

Neuropil pruning in Early-Course Schizophrenia: Immunological, Clinical, and Neurocognitive Correlates

Konasale M. Prasad[1,*], **Ashley M. Burgess**[2], **Matcheri S. Keshavan**[3], **Vishwajit L. Nimgaonkar**[1], and **Jeffrey A. Stanley**[2]

[1]University of Pittsburgh School of Medicine, Pittsburgh, PA 15143

[2]Wayne State University School of Medicine, Detroit, MI

[3]Beth Israel Deaconess Medical Center, Harvard Medical School, Boston, MA

Abstract

Introduction—Neuropathological studies suggest neuropil reduction in schizophrenia. Altered synaptic pruning is proposed to underlie neuropil reduction. Underlying factors and clinical correlates of synaptic pruning are poorly understood. Using phosphorus magnetic resonance spectroscopy (^{31}P MRS), it is feasible to assess membrane phospholipid (MPL) metabolites in the brain that specifically and sensitively reflect neuropil expansion (elevated MPL precursors) or contraction (elevated MPL catabolites).

Methods—We examined MPL metabolites and their cognitive, clinical and immunologic correlates among 28 early-course schizophrenia individuals (illness duration 1.99±1.33 years; antipsychotic-naïve=18) and 21 controls. We acquired whole-brain multi-voxel ^{31}P MRS data from 12 unique brain regions. Interleukin-6 and C-reactive protein (CRP) were assayed in the serum. Generalized linear mixed models examined case-control differences in MPL metabolites in these regions correcting for multiple testing. Partial correlations accounting for multiple tests examined the relationship of Interleukin-6 and CRP levels with MPL metabolite levels.

Results—MPL catabolite levels were increased in the thalamus in schizophrenia compared to controls. Interleukin-6 and CRP levels did not show case-control differences. Interleukin-6 levels positively correlated with MPL catabolite levels in the thalamus after correcting for multiple tests. The left thalamus MPL catabolite levels correlated negatively with sustained attention (corrected p=0.039).

Discussion—Elevated MPL catabolites in the thalamus suggest increased neuropil contraction that may be related to excessive synaptic pruning. The thalamic neuropil contraction is associated with Interleukin-6 levels suggesting central pathogenic mechanisms for the inflammatory

[*]Corresponding Author: Ste 431, 3811 O'Hara St, Pittsburgh, PA 15143, PrasadKM@upmc.edu.

A version of this data was presented at the American College of Neuropsychopharmacology meeting at Hollywood, FL Dec 3–6, 2015

Conflict of Interest

All authors report no biomedical financial interests or potential conflicts of interest.

mediators. Correlation of increased thalamic MPL catabolite levels with cognitive impairments suggests clinical correlates of neuropil contraction.

Keywords

Inflammation; Cytokines; Schizophrenia; Magnetic Resonance Spectroscopy; Neuropil; Cognitive performance

INTRODUCTION

Changes in gray matter volumes, and cortical thickness and surface area are extensively reported in schizophrenia (1). Gray matter metrics represent a composite measure of axons, dendrites, synapses, glia, neuronal soma, interneurons, interneuronal space and microvasculature (2), and hence, do not reflect pathology in the neuropil, which is defined as synaptically dense region of dendrites, unmyelinated axons and glia with few cell bodies (3, 4). Phosphorus magnetic resonance spectroscopy (^{31}P MRS) can more specifically assess neuropil by measuring membrane phospholipid (MPL) precursors [phosphocholine, PC; phosphoethanolamine, PE] and catabolites [glycerophosphocholine, GPC; glycerophosphoethanolamine, GPE].

The MPL's (phosphatidylcholine, PtdC; phosphatidylethanolamine, PtdE) are an integral part of neuronal and glial membrane bilayers. Expansion/contraction of cell membranes that primarily occurs at the axonal endings and dendritic branches during neuropil growth/pruning are associated with elevated MPL precursors (PE, PC) or catabolites (GPC, GPE), respectively. Changes in myelination, neuronal somal size and glial cells contribute considerably less to MPL metabolite signals on ^{31}P MRS (5). For these reasons, major source of MPL metabolite signals is the synaptically dense neuropil (6, 7). Specificity of MPL measures to neuropil pruning/formation is supported by animal lesion (5), cellular model (8), human postmortem (9) and neurodevelopmental (10, 11) data. Elevated PE+PC are noted at the time and site of neuropil growth that increases the demand to produce MPLs (5, 10, 11); likewise increased GPC and GPE is related to pruning (5, 12). Striking changes in MPL metabolites emerged well before gray matter changes in a large cohort of healthy children/adolescents suggesting greater sensitivity of ^{31}P MRS measures (11, 13). Thus, it is feasible to more specifically conduct in vivo examination of neuropil pathology using ^{31}P MRS in schizophrenia.

Factors that contribute to neuropil pathology in schizophrenia is poorly understood. Inflammatory mediators are associated with synaptic pruning and formation (14). Mounting data support the association of inflammation with schizophrenia (15–17). Postmortem studies report activated microglia/macrophages (18, 19), elevated expression of inflammatory markers in the prefrontal neurons (20) and vasculature (21), and autoantibodies against frontal (22), cingulate (23), hippocampal cortices (24), and glutamate receptors (25) in schizophrenia. Autoimmune disorders may elevate schizophrenia risk both independently (26) and in combination with infections (26). A meta-analysis noted elevated peripheral blood inflammatory cytokines in schizophrenia compared to controls (27, 28). Genome-wide association studies have replicated the association of the Major

Histocompatibility Complex (MHC) region variants, where a large number of immune genes are located, with schizophrenia (29–31). Potential gene-environmental interactions on gray matter changes in schizophrenia is also reported (32).

Newer data in schizophrenia, including ours, associate inflammation with cognitive deficits (33, 34), severity of psychopathology (35) and anatomical dysconnections (36, 37). However, there are no studies on the association of inflammation with changes in neuropil in schizophrenia. Gray matter loss was associated with peripheral blood interleukin-6 (IL-6) levels in healthy middle-aged adults (38). Enhanced progressive cortical thickness reduction in clinical high risk subjects correlated with peripheral inflammatory mediator levels suggesting that inflammation may increase schizophrenia risk (39).

Among the peripheral inflammatory markers, IL-6 and C-reactive protein (CRP) levels are more extensively examined in schizophrenia. IL-6 is predominantly a pro-inflammatory cytokine secreted by T-cells and macrophages (40). CRP is a phylogenetically highly conserved acute phase reactant and a pattern recognition molecule that is primarily expressed in liver following induction by IL-6(41). Although extra-hepatic expression of CRP in the neurons (42) and lymphocytes (43) are described, plasma levels mainly reflect hepatic synthesis (41). CRP may be either pro- or anti-inflammatory, depending on the context (44). Meta-analyses report elevated IL-6 (27) and CRP (28) levels in schizophrenia with variations related to antipsychotic use, comorbidities and illness stage.

We examined MPL metabolite levels in specific brain regions across the entire brain in early-course schizophrenia compared to controls, and the relationship of MPL metabolite variations with IL-6 and CRP levels, performance on sustained attention, executive function and verbal memory tasks, and severity of psychopathology. We hypothesized that the GPC +GPE would be elevated and/or PC+PE would be decreased in key regions such as the prefrontal cortex, hippocampus, striatum and thalamus in schizophrenia compared to controls. We, further, hypothesized that the IL-6 and CRP levels would positively correlate with GPE+GPC levels that index neuropil pruning and/or negatively with PC+PE that indexes neuropil synthesis based on the association of inflammatory mediators with smaller hippocampus (38). We predicted that the severity of psychopathology would be positively correlated with MPL catabolites and/or negatively with MPL precursors.

METHODS

Clinical Evaluations

We enrolled 49 young adults (SZ=28, CONTROLS=21) with DSM-IV schizophrenia/ schizoaffective disorder between 18–40 years old and with an illness duration of less than 5 years from the onset of first psychotic symptom from outpatient services of the University of Pittsburgh Medical Center. The diagnosis was confirmed by administering the Structured Clinical Interview for DSM diagnosis (SCID-IV) (45) and through consensus diagnosis by experienced diagnosticians (46). Total antipsychotic dose and treatment duration were also collected. Substance abuse in the previous month or dependence 6 months prior to enrolment, mental retardation per DSM-IV, serious neurological/medical illnesses were exclusion criteria.

Psychopathological and Neurocognitive assessments

The psychopathology was rated on the Brief Psychiatric Rating Scale (BPRS) (47), the Schedules for the Assessment of Positive Symptoms (SAPS)(48) and the Schedules for the Assessment of Negative Symptoms (SANS) (49). Sustained attention, executive functions and verbal memory were evaluated within a week of imaging using the Go-No-Go test, the Wisconsin Card Sorting Test (WCST) and the Word List Memory Test (WLMT), respectively. Accuracy and response times were used to examine sustained attention. We used perseverative error percentages on the WCST to index executive functions, and trial-to-trial transfer for verbal memory and learning within the WLMT.

Imaging procedures

Whole-brain, multi-voxel, in vivo ^{31}P MRS data in 3-dimensions was collected on a 3T Siemens Tim Trio system using a dual-tuned ^{1}H-^{31}P volume head coil. The acquisition approach used the conventional chemical shift imaging (CSI) sequence, which used a single slice-selective excitation pulse to define a large axial slab and phase encoding gradients in all three directions (termed FID_CSI on the Siemens system). Acquisition parameters were: FOV=310×310×160mm, acquired phase encoding steps=14×14×8 and zero-filled to 16×16×8 (nominal voxel dimension=1.94×1.94×2.0cm^3), TR=0.54sec, flip-angle=33^0 reflecting the Ernst angle where the average T_1 value of phosphocreatine (PCr), PE, PC was 3 sec, complex data points=2,048, spectral bandwidth=4.0kHz, 24 averages of the CSI matrix in which the averaging was weighted to the central k-space points conforming to a 3D elliptical function and pre-acquisition delay time of 1.4ms. T_1-weighted MPRAGE images were collected and used in the post-processing to guide the extraction of ^{31}P MRS signal of 12 unique voxels-of-interest on both sides placed in anatomically specific regions, namely the dorsolateral (DLPFC) and ventral prefrontal cortex, inferior frontal cortex, ventral and dorsal hippocampus, striatum, thalamus, anterior, middle and posterior cingulate, superior temporal gyrus and inferior parietal lobule.

The voxels-of-interest were predefined anatomically on a template brain and by co-registering the subject's T_1-weighted images to the template brain (12 degrees of freedom) and re-mapping the voxels to the subject space via the inverse transformation (50). The coordinate of each voxel location in subject space were then used to mathematically shift the 3D multi-voxel grid (i.e., by applying a phase shift in the k-space) to ensure the ^{31}P MRS voxel was centered at each location before extracting the ^{31}P MRS signal for quantification. This highly innovative procedure ensured that the voxel placements were consistently and systematically placed in the specified anatomical locations between subjects, and is demonstrated to be highly accurate and reliable (50).

In the *k*-space domain of the ^{31}P MRS data, a 75% Hamming window was applied, which collectively with the phase-encoding steps, elliptical weighted sampling of the k-space and k-space filter, resulted in estimated effective voxel size of ≈20cm^3. The extracted ^{31}P signals were apodized (5Hz Gaussian) and modeled in the time domain with 23 Gaussian-damped sinusoids [PE, PC, GPE and GPC as triplets, Pi, MPL_{broad}, PCr and dinucleotides as singlets, and adenosine triphosphate (ATP) (two doublets and a triplet)]. The post-processing and metabolite quantification of extracted ^{31}P MRS signal was 100% automated (50).

Metabolite levels were expressed as a percentage of the total signal (i.e., mole%). Due to the lack of ^{1}H decoupling, the quantification of the individual phosphomonoesters (PE and PC), and phosphodiesters (GPE and GPC) were indistinguishable. Therefore, summated measures (PE+PC, GPE+GPC) were obtained.

The proportion of gray and white matter, and CSF/extra-cortical space was estimated for each voxel-of-interest, again, using a fully automated procedure. A B1-field bias correction was applied to the T_1-weighted MRI followed by extracting the brain tissue and segmenting the images into partial volume maps of gray and white matter tissue, and CSF/extracortical space using FreeSurfer and FSL tools (e.g. FLIRT, NU_CORRECT, BET and FAST) (51–53). Since the CSF concentration of ^{31}P metabolites is below the detection limit and the ^{31}P metabolites are expressed as a percentage relative to the total signal, the correction for CSF fractions is not applicable and do not confound the ^{31}P MRS results.

Immunological Assays

IL-6 and CRP were assayed in duplicates on the peripheral blood collected around the same time of the day from all subjects using quantitative ultrasensitive and highly specific magnetic bead immunoassay at the University of Pittsburgh Luminex facility. Polystyrene microsphere beads that are internally dyed with red and infrared fluorospheres of differing fluorescence signal intensities were read using Luminex detection systems, after sandwich immunoassay. Results were reported using an industry-recommended 5-place standard curve with a recovery percentage range for the curve (between 70%-130%). Excluding the samples outside of this range, good quality CRP data was obtained on 26 schizophrenia subjects and 19 controls, and for IL-6 on 25 schizophrenia subjects and 16 controls. The curve fit ranged between 98 and 104 for the included samples. There were no significant differences between subjects with good quality and poor quality IL-6 or CRP data.

Statistical Plan

The data were largely normally distributed. We preferred multivariate modeling using generalized linear mixed model to examine case-control differences in MPL metabolites because the metabolite levels from the voxels-of-interest were correlated with each other, and to reduce the number of univariate comparisons (12 voxels*2 sides*2 metabolites). One model was built for each metabolite (PC+PE and GPC+GPE). Each model included all voxels-of-interest on both sides as repeated measures controlling for age, sex and the gray matter fraction of each voxel. For multiple comparison corrections, we used a highly conservative sequential Bonferroni correction within each model that accounted for the number of voxels-of-interest and hemisphere. Since one model was built for each metabolite, correction for metabolites were applied post-hoc. To address relatively small sample that was unbalanced between schizophrenia and controls, we used the Satterthwaite approximation that estimated pooled degrees of freedom, and robust estimation for handling violations of model assumptions that are true for large sample sizes. Significance for the overall model for each metabolite and post-hoc corrected significance for each voxel-of-interest are reported. Unstandardized B values and standardized effect sizes (Cohen's *d*) are reported for the diagnosis main effects on MPL metabolites.

Because of non-normal distribution, log-transformed IL-6 and CRP levels were used in partial correlation tests to examine their relationship with PC+PE and GPC+GPE levels from each voxel including age, sex and diagnostic group as covariates. Locally Weighted Scatterplot Smoothing (LOWESS) regressions using triweight approach to weight each *k*-nearest neighbor as a curve fitting method examined the best fit for the correlation of IL-6 and CRP levels with GPC+GPE and PC+PE.

We, next, selected the voxels that survived multiple test corrections for correlations of MPL metabolites with IL-6 and CRP to examine their relationship with psychopathological and neurocognitive measures. Depending on the number of voxels included in correlation tests, Bonferroni corrections were applied.

RESULTS

Demographic and Clinical

Schizophrenia and control subjects did not differ in age (p=0.97). Sex distribution was significantly different (χ^2=7.89, p=0.009). Mean illness duration was 1.99±1.33 years from the onset of psychotic symptoms. Eighteen schizophrenia subjects were medication-naïve while 10 were treated with second generation antipsychotics (mean dose=317.53±270.20 mg chlorpromazine equivalent for 488.93±320.71 mean number of days); 6 of these patients also received other psychotropics, e.g. lithium, antidepressants (Table 1).

Quality of ^{31}P MRS data

Repeated measures ANOVA that included all voxels-of-interest did not show significant diagnosis*hemisphere interaction. Since the data violated sphericity assumptions, the conservative Greenhouse-Geisser method was used to correct the degrees-of-freedom. The overall mean signal-to-noise ratio of PCr for the 12 voxels-of-interest of patients (3.37±0.45) and controls (3.76±1.05) (where noise was defined as the root-mean-square of the noise) (F(3.65–127.89)=0.65, p=0.61), the mean Gaussian linewidths of the PCr (Schizophrenia: 10.77±3.24 Hz; Control: 12.17±4.26 Hz) (F(4.19–146.54)=0.90, p=0.47) and the Cramer-Rao Lower Bound values for PC+PE (Schizophrenia: 12.69±4.05, Controls: 12.43±3.86) (F(1.0–32.0)=0.008, p=0.93) and GPC+GPE (16.44±8.23, Controls: 20.03±14.84); (F(1.34–40.20)=1.48, p=0.24) did not show between-group differences (Fig 1).

Diagnosis main effects

Diagnosis-by-hemisphere interaction for both metabolites was not significant (both p>0.35). Diagnosis main effects on GPC+GPE levels were observed at the thalamus, DLPFC, ventral hippocampus, inferior frontal cortex, inferior parietal lobule and superior temporal gyrus (Overall model, F(24, 614)=8.19, p<0.001). GPC+GPE levels were elevated in bilateral thalamus and right ventral hippocampus but reduced in the right DLPFC and inferior frontal cortex, and bilateral inferior parietal lobule, superior temporal gyrus in schizophrenia compared to controls (Table 1) (Fig 1). The ventral prefrontal cortex, bilateral dorsal hippocampus, bilateral striatum, and cingulate did not show diagnosis effect.

The diagnosis main effects on PC+PE levels was also significant (F(24, 628)=12.79, p<0.001). The PC+PE levels were elevated in schizophrenia compared to controls in bilateral ventral and the dorsal hippocampus, and in the left anterior cingulate cortex. PC +PE was reduced in bilateral inferior frontal cortex and left inferior parietal lobule. The ventral prefrontal cortex, left DLPFC, bilateral thalamus and superior temporal gyrus, the right inferior parietal lobule, bilateral striatum and cingulate did not show diagnosis effect on PC+PE.

Antipsychotic use did not show main effect on either GPC+GPE (p=0.8) or PC+PE (p=0.07). Effect sizes (Cohen's *d*) were small to medium for diagnosis effect on MPL metabolites variations (Table 1).

Correlation of MPL metabolites with IL-6 and CRP levels

IL-6 and CRP levels did not show significant case-control differences (Table 1). IL-6 levels positively correlated with GPC+GPE levels in bilateral thalamus (Right, r=0.47, p=0.005; Left, r=0.57, p=0.0004), the left dorsal hippocampus (r=0.44, p=0.009) and the left dorsal anterior cingulate (0.37, p=0.028). Correlation of IL-6 levels with left thalamus GPC+GPE survived multiple test correction (12 voxels*2sides*2 immune mediators) (corrected p=0.0192). Since the correlation of immune mediators with PC+PE and GPC+GPE were tested as two separate hypotheses, we did not correct for the number of metabolites. However, IL-6 significantly correlated with left thalamus GPC+GPE even after correcting for number of metabolites (12 voxels*2sides*2 immune mediators*2 MPL metabolites=96 tests, corrected p=0.0384). LOWESS regression showed elevated GPC+GPE levels at relatively lower IL-6 levels in schizophrenia compared to controls. At higher IL-6 levels, both schizophrenia and controls showed similar GPC+GPE elevations (Fig 2).

CRP levels correlated negatively with PC+PE in the left striatum (r=-0.38, p=0.02), mid-anterior cingulate (r=-0.38, p=0.025), the left dorsal anterior cingulate (r=-0.38, p=0.024) and ventral prefrontal cortex (r=-0.44, p=0.025). These correlations did not survive multiple test corrections. None of these voxels showed diagnosis main effects.

Correlation of MPL metabolites, IL-6 and CRP levels with psychopathology and neurocognition

The left thalamus GPC+GPE correlated positively with negative symptoms (r=0.44, p=0.008); after excluding an outlier, it was not significant (r=0.23, p=0.2). The left thalamus GPC+GPE positively correlated with Go-No-Go response time (r=0.26, p=0.013) but negatively with verbal learning (r=—0.21, p=0.04). The correlation of Go-No-Go response time survived multiple test corrections (1 voxel*1 metabolite*3 cognitive domains, corrected p=0.039) and verbal learning remains a trend. CRP levels did not correlate with psychopathology or neurocognitive measures (Fig 3). Positive symptom severity and WCST performance did not correlate with MPL metabolite, IL-6 or CRP levels. An exploratory pathway analysis showed a trend (p=0.09) for "indirect effect" of IL-6 on negative symptoms and sustained attention through GPE+GPC levels in the thalamus. The "direct effect" of IL-6 on severity of psychopathology and cognitive performance was not significant.

DISCUSSION

This is the first whole-brain multi-voxel ^{31}P MRS study in early-course schizophrenia with a mean illness duration less than 2 years. We observed a robust increase in MPL *breakdown products* in the thalamus and in MPL *precursors* in the hippocampus in schizophrenia compared to controls. Interestingly, neocortical voxels showed reduction in both GPC+GPE and PC+PE. Higher thalamic GPC+GPE correlated with IL-6 levels and sustained attention deficits after correcting for multiple tests. The hippocampus mainly showed increased PC +PE; however, increased PC+PE and GPC+GPE in the right ventral hippocampus suggest increased neuropil turnover.

A seminal ^{31}P MRS study at 1.5 Tesla (54) provided the first direct in vivo evidence of altered neuropil development suggested by decreased PC+PE and increased GPC+GPE in first-episode neuroleptic-naïve schizophrenia which was later supported by postmortem neuropil morphology data (55–57). Another neuroleptic-naïve schizophrenia study showed increased PDE/PME ratio in the basal ganglia (58). Our study does not replicate both these findings that examined 1.5T ^{31}P data. Our data was from more powerful 3T scanner on early-course patients of whom nearly two-thirds were medication-naïve. Results are inconsistent among medicated and chronic schizophrenia, e.g. higher GPC+GPE in the frontal (59) and temporal regions (60), and decreased GPE in bilateral frontal lobes (61), anterior cingulate and left thalamus (62). Such inconsistencies may be due to heterogeneity of the illness and its progression, regional heterogeneity in pathology, medications, comorbidity, scanner resolutions, and voxel size and number. Our observations suggest that the inflammatory state may also contribute to such inconsistencies.

Two-thirds of our patients were antipsychotic-naïve. The data is likely to be reliable because of a short duration of illness (<2 years) and treatment (median duration≈45 days), and collection of medication data from multiple sources (self-reports, electronic and pharmacy records). However, the entire history of psychotropic data was not available. Extensive literature review suggests more consistent changes in ATP and PCr but fewer alterations in MPL metabolites following both atypical and typical neuroleptics administration. MPL metabolite changes were noted after short-term (63, 64) but not long-term (65) antipsychotic treatment. The neuroleptic dose in schizophrenia correlated with ATP and PCr/ATP ratio but not MPL metabolites (66). Most of these studies were conducted on small samples using 2D ^{31}P MRS at 1.5 T with large voxels. Since more patients were antipsychotic-naïve, antipsychotic-treatment duration was short and the main effect of antipsychotics was not statistically significant, observed association of MPL metabolites with schizophrenia, and its correlation with IL-6 and sustained attention may not be significantly influenced by medications. Because of short illness duration, illness chronicity may not have significantly contributed to our observations.

Increased GPC+GPE in the thalamus suggest excessive neuropil pruning. Concurrently elevated GPC+GPE and decreased PC+PE was not observed in any voxel-of-interest. Elevated GPC+GPE along with no significant PC+PE change may still suggest increased neuropil pruning. Expansion/contraction of neuronal membrane requires synthesis/ breakdown, respectively, of MPLs (PtdC and PtdE). Neuronal membranes expand/contract

primarily at the axonal endings and dendritic branches during neuropil growth/pruning, the magnitude of which is considerably higher than that in the neuronal soma, glia and myelin. Hence, the contribution of MPL synthesis/breakdown at the axonal endings and dendritic branches to MPL metabolite levels is proportionately high (5). For example, dendritic and axonal arborizations contribute the most to membrane surface area in a typical neuron of ~250,000 μm^2 compared to a spherical cell of 20 μm diameter and surface area of 1256 μm^2 (67). During development, a neuronal soma of 50 μm diameter increase by 0.6% in volume/day compared to 20% increase/day in surface area (6) through formation of synapses and dendritic arborizations resulting in gain of membranes, reflected in elevated PC+PE. Similarly, membrane loss primarily occurs during synaptic pruning, which is indexed by elevated GPC+GPE. Convergent data from animal (5, 68), postmortem (9, 69) and human developmental (11, 12) studies suggest associations between elevated GPC+GPE and neuropil pruning. In vivo human (11, 70, 71) and ex vivo rat brain extract (12, 72) ^{31}P MRS data consistently show correlation of high PE+PC levels and low GPC+GPE levels with neuritogenesis and brain electrical activity(70). Rat studies show elevated PC+PE associated with growth spurts and rapid neuropil changes concomitant with increased PtdC at the time and site of neurite growth (ipsilateral side of the lesion) during recovery from unilateral lesions of the entorhinal cortex (5, 68). Decreased PC+PE and increased GPC+GPE reflecting synaptic pruning is also observed as the brain matures(72). Cellular studies observed PC elevation within 60 minutes of neuritogenesis(8). ^{31}P MRS studies are important because human studies failed to correlate gray matter density/volume changes on T_1-weighted structural MRI acquired on both 1.5T (73) and 3T (74) scanners with histopathologically measured neuronal density. ^{31}P MRS can more specifically measure neuropil that is pathophysiologically more relevant.

Prior studies show smaller thalamus volume in schizophrenia (75–77) that correlated with both negative and positive symptoms (76) and cognitive performance (78). Correlation of impaired sustained attention (increased Go-No-Go response time) underscores the clinical significance of increased thalamic pruning. Prior studies report correlation of elevated temporal lobe GPC+GPE with positive symptom severity (60). Correlation of WCST results with PC+PE in schizophrenia (79) is not replicated (80).

Plausible mechanisms linking inflammation with neuropil loss merit discussion. Immune mediators may affect synaptic pruning and formation (14), especially during neurodevelopment(81). Cytokines, including IL-6, modulate synaptic plasticity and neurotransmission (82). Schizophrenia-associated Human Leukocyte Antigen (HLA) gene variations are associated with smaller thalamus (83). Further, reciprocal regulation between immune and neurotransmitter systems suggests additional pathways. Cytokines (84, 85) and chemokines (86) receptors on neurons and glia affect signal transduction (87), and neurotransmission via dopamine(88), glutamate(89), serotonin (90) and norepinephrine (91). Interleukin-1 receptor type I (IL-1RI) is enriched at synaptic sites where it co-localizes with NMDA receptors and modulates NMDA activation through IL-1β (a pro-inflammatory cytokine) (85); interferon-α (IFN-α) decreases dopamine and serotonin biosynthesis (88). Likewise, dopamine modulates immune cell activity (92–94). Cytokines, including IL-6 may interact with complement cascades and regulate synaptic pruning (14).

The importance of peripheral blood IL-6 for the central nervous system physiology is debated. Peripheral blood IL-6 may access brain through a leaky blood brain barrier (95) or through a specific transport mechanism even with intact blood brain barrier (96). Further, brain may be a source of peripheral blood IL-6 (97). Contribution of immune mediators in different tissue compartments to pathophysiology of schizophrenia needs more research; our study is a step in that direction.

Correlation of IL-6 with MPL metabolites without significant case-control differences suggest increased susceptibility of schizophrenia subjects for peripheral inflammatory mediators. It is unclear why thalamus but no other regions showed correlation of MPL metabolites with elevated IL-6 levels. An extensive literature review could not find differential distribution of IL-6 immunoreactive neurons in the thalamus. Animal studies do not show elevated cytokine gene expression in the thalamus following intraperitoneal lipopolysaccharide injection (98). Future studies should focus on these issues since pathophysiological significance of inflammation in schizophrenia is poorly understood. Lack of correlation of CRP with GPC+GPE is notable. Adequately powered sample may reveal differences.

Our study highlights a potentially treatable mechanism underlying cognitive impairments in schizophrenia. Strengths of the study include case ascertainment through experienced clinician consensus, examination of 12 unique regions often associated with schizophrenia, higher specificity of ^{31}P MRS measures to neuropil, examination of IL-6 and CRP levels using state-of-the art, highly sensitive assays with good quality control on peripheral blood collected around the same time of the day to minimize diurnal variations.

Limitations include relatively small sample and examination of two immune mediators. Smoking data was not available to covary. Scanner resolution at 3 Tesla, although better than 1.5T, could improve by more than 4 times for the peripheral voxels and by 50% for the central voxels at 7 Tesla (99) to resolve individual metabolites for examination. Examining larger samples using a comprehensive immune mediator panel could highlight the impact of pro-inflammatory versus anti-inflammatory effects on neuropil. We obtained gray matter, white matter and cerebrospinal fluid proportions for each voxel but did not calculate the proportion of each structure-of-interest vs non-structure-of-interest in the voxel.

Acknowledgments

This work was supported by research grants from the National Institute of Mental Health MH72995, and MH93540 (KMP). We thank Dr. Debra Montrose, Dr. Elizabeth Radomsky, Mr. Kevin Eklund, Ms. Diana Dworakowski and Ms. Alicia Thomas for enrolment and characterization of research participants. We also thank Mr. Dhruman Goradia, Ms, Krishna Pancholi, Mr. Steven Goodnow, Ms. Jean Miewald and Ms. Karol Rosengarth for their help in data analysis, data management and quality assurance. Funding agencies did not have any further role in the analysis and reporting of the results.

REFERENCES

1. Shenton ME, Dickey CD, Frumin M, McCarley RW. A review of MRI findings in schizophrenia. Schizophr Res. 2001; 49:1–52.
2. Weinberger DR, Radulescu E. Finding the Elusive Psychiatric “Lesion” With 21st-Century Neuroanatomy: A Note of Caution. Am J Psychiatry. 2016; 173:27–33. [PubMed: 26315983]

3. Kandel, ER. Principles of neural science. 5th. New York: McGraw-Hill; 2013.
4. Gazzaniga, MS. The cognitive neurosciences. 4th. Cambridge, Mass: MIT Press; 2009.
5. Geddes JW, Panchalingam K, Keller JN, Pettegrew JW. Elevated phosphocholine and phosphatidylcholine following rat entorhinal cortex lesions. Neurobiol Aging. 1997; 18:305–308. [PubMed: 9263196]
6. Pfenninger KH. Plasma membrane expansion: a neuron's Herculean task. Nat Rev Neurosci. 2009; 10:251–261. [PubMed: 19259102]
7. Pfenninger KH, Johnson MP. Membrane biogenesis in the sprouting neuron. I. Selective transfer of newly synthesized phospholipid into the growing neurite. The Journal of cell biology. 1983; 97:1038–1042. [PubMed: 6194160]
8. Marcucci H, Paoletti L, Jackowski S, Banchio C. Phosphatidylcholine biosynthesis during neuronal differentiation and its role in cell fate determination. J Biol Chem. 2010; 285:25382–25393. [PubMed: 20525991]
9. O'Brien JS, Sampson EL. Lipid composition of the normal human brain: gray matter, white matter, and myelin. Journal of lipid research. 1965; 6:537–544. [PubMed: 5865382]
10. Pettegrew JW, Klunk WE, Panchalingam K, McClure RJ, Stanley JA. Molecular insights into neurodevelopmental and neurodegenerative diseases. Brain Res Bull. 2000; 53:455–469. [PubMed: 11137004]
11. Stanley JA, Kipp H, Greisenegger E, MacMaster FP, Panchalingam K, Keshavan MS, et al. Evidence of developmental alterations in cortical and subcortical regions of children with attention-deficit/hyperactivity disorder: a multivoxel in vivo phosphorus 31 spectroscopy study. Arch Gen Psychiatry. 2008; 65:1419–1428. [PubMed: 19047529]
12. Pettegrew JW, Kopp SJ, Minshew NJ, Glonek T, Feliksik JM, Tow JP, et al. 31P nuclear magnetic resonance studies of phosphoglyceride metabolism in developing and degenerating brain: preliminary observations. J Neuropathol Exp Neurol. 1987; 46:419–430. [PubMed: 2955082]
13. Goldstein G, Panchalingam K, McClure RJ, Stanley JA, Calhoun VD, Pearlson GD, et al. Molecular neurodevelopment: an in vivo 31P-1H MRSI study. J Int Neuropsychol Soc. 2009; 15:671–683. [PubMed: 19674503]
14. Stephan AH, Barres BA, Stevens B. The complement system: an unexpected role in synaptic pruning during development and disease. Annu Rev Neurosci. 2012; 35:369–389. [PubMed: 22715882]
15. Muller N, Schwarz MJ. Immune System and Schizophrenia. Current immunology reviews. 2010; 6:213–220. [PubMed: 21057585]
16. Meyer U, Weiner I, McAlonan GM, Feldon J. The neuropathological contribution of prenatal inflammation to schizophrenia. Expert Rev Neurother. 2011; 11:29–32. [PubMed: 21158552]
17. Saetre P, Emilsson L, Axelsson E, Kreuger J, Lindholm E, Jazin E. Inflammation-related genes up-regulated in schizophrenia brains. BMC Psychiatry. 2007; 7:46. [PubMed: 17822540]
18. Bayer TA, Buslei R, Havas L, Falkai P. Evidence for activation of microglia in patients with psychiatric illnesses. Neurosci Lett. 1999; 271:126–128. [PubMed: 10477118]
19. Radewicz K, Garey LJ, Gentleman SM, Reynolds R. Increase in HLA-DR immunoreactive microglia in frontal and temporal cortex of chronic schizophrenics. J Neuropathol Exp Neurol. 2000; 59:137–150. [PubMed: 10749103]
20. Fillman SG, Cloonan N, Catts VS, Miller LC, Wong J, McCrossin T, et al. Increased inflammatory markers identified in the dorsolateral prefrontal cortex of individuals with schizophrenia. Mol Psychiatry. 2013; 18:206–214. [PubMed: 22869038]
21. Harris LW, Wayland M, Lan M, Ryan M, Giger T, Lockstone H, et al. The cerebral microvasculature in schizophrenia: a laser capture microdissection study. PLoS ONE. 2008; 3:e3964. [PubMed: 19088852]
22. Henneberg AE, Horter S, Ruffert S. Increased prevalence of antibrain antibodies in the sera from schizophrenic patients. Schizophr Res. 1994; 14:15–22. [PubMed: 7893617]
23. Kelly RH, Ganguli R, Rabin BS. Antibody to discrete areas of the brain in normal individuals and patients with schizophrenia. Biol Psychiatry. 1987; 22:1488–1491. [PubMed: 3676378]

24. Ganguli R, Rabin BS, Kelly RH, Lyte M, Ragu U. Clinical and laboratory evidence of autoimmunity in acute schizophrenia. Ann N Y Acad Sci. 1987; 496:676–685. [PubMed: 3474998]
25. Tsutsui K, Kanbayashi T, Tanaka K, Boku S, Ito W, Tokunaga J, et al. Anti-NMDA-receptor antibody detected in encephalitis, schizophrenia, and narcolepsy with psychotic features. BMC Psychiatry. 2012; 12:37. [PubMed: 22569157]
26. Benros ME, Nielsen PR, Nordentoft M, Eaton WW, Dalton SO, Mortensen PB. Autoimmune diseases and severe infections as risk factors for schizophrenia: a 30-year population-based register study. Am J Psychiatry. 2011; 168:1303–1310. [PubMed: 22193673]
27. Miller BJ, Buckley P, Seabolt W, Mellor A, Kirkpatrick B. Meta-analysis of cytokine alterations in schizophrenia: clinical status and antipsychotic effects. Biol Psychiatry. 2011; 70:663–671. [PubMed: 21641581]
28. Miller BJ, Culpepper N, Rapaport MH. C-Reactive Protein Levels in Schizophrenia: A review and meta-analysis. Clinical Schizophrenia & Related Psychoses. 2014; 7:223–230. [PubMed: 23428789]
29. Shi J, Levinson DF, Duan J, Sanders AR, Zheng Y, Pe'er I, et al. Common variants on chromosome 6p22.1 are associated with schizophrenia. Nature. 2009; 460:753–757. [PubMed: 19571809]
30. Stefansson H, Ophoff RA, Steinberg S, Andreassen OA, Cichon S, Rujescu D, et al. Common variants conferring risk of schizophrenia. Nature. 2009; 460:744–747. [PubMed: 19571808]
31. Sekar A, Bialas AR, de Rivera H, Davis A, Hammond TR, Kamitaki N, et al. Schizophrenia risk from complex variation of complement component 4. Nature. 2016; 530:177–183. [PubMed: 26814963]
32. Prasad KM, Bamne MN, Shirts BH, Goradia D, Mannali V, Pancholi KM, et al. Grey matter changes associated with host genetic variation and exposure to Herpes Simplex Virus 1 (HSV1) in first episode schizophrenia. Schizophr Res. 2010; 118:232–239. [PubMed: 20138739]
33. Ribeiro-Santos A, Lucio Teixeira A, Salgado JV. Evidence for an immune role on cognition in schizophrenia: a systematic review. Current neuropharmacology. 2014; 12:273–280. [PubMed: 24851091]
34. Fineberg AM, Ellman LM. Inflammatory cytokines and neurological and neurocognitive alterations in the course of schizophrenia. Biol Psychiatry. 2013; 73:951–966. [PubMed: 23414821]
35. Takano A, Arakawa R, Ito H, Tateno A, Takahashi H, Matsumoto R, et al. Peripheral benzodiazepine receptors in patients with chronic schizophrenia: a PET study with [11C]DAA1106. Int J Neuropsychopharmacol. 2010; 13:943–950. [PubMed: 20350336]
36. Prasad KM, Upton CH, Nimgaonkar VL, Keshavan MS. Differential susceptibility of white matter tracts to inflammatory mediators in schizophrenia: An integrated DTI study. Schizophr Res. 2015; 161:119–125. [PubMed: 25449712]
37. Najjar S, Pearlman DM. Neuroinflammation and white matter pathology in schizophrenia: systematic review. Schizophr Res. 2015; 161:102–112. [PubMed: 24948485]
38. Marsland AL, Gianaros PJ, Abramowitch SM, Manuck SB, Hariri AR. Interleukin-6 covaries inversely with hippocampal grey matter volume in middle-aged adults. Biol Psychiatry. 2008; 64:484–490. [PubMed: 18514163]
39. Cannon TD, Chung Y, He G, Sun D, Jacobson A, van Erp TG, et al. Progressive reduction in cortical thickness as psychosis develops: a multisite longitudinal neuroimaging study of youth at elevated clinical risk. Biol Psychiatry. 2015; 77:147–157. [PubMed: 25034946]
40. Kato A, Watanabe T, Yamazaki M, Deki T, Suzuki M. IL-6R distribution in normal human and cynomolgus monkey tissues. Regulatory toxicology and pharmacology : RTP. 2009; 53:46–51. [PubMed: 19010373]
41. Black S, Kushner I, Samols D. C-reactive Protein. J Biol Chem. 2004; 279:48487–48490. [PubMed: 15337754]
42. Yasojima K, Schwab C, McGeer EG, McGeer PL. Human neurons generate C-reactive protein and amyloid P: upregulation in Alzheimer's disease. Brain Res. 2000; 887:80–89. [PubMed: 11134592]

43. Kuta AE, Baum LL. C-reactive protein is produced by a small number of normal human peripheral blood lymphocytes. The Journal of experimental medicine. 1986; 164:321–326. [PubMed: 3723078]
44. Eisenhardt SU, Thiele JR, Bannasch H, Stark GB, Peter K. C-reactive protein: how conformational changes influence inflammatory properties. Cell Cycle. 2009; 8:3885–3892. [PubMed: 19887916]
45. First, MB. The Structured Clinical Interview for DSM-IV for Axis I disorders: Clinical Version, Administration Booklet. Washington, DC: American Psychiatric Press; 1997.
46. Stolz E, Pancholi KM, Goradia DD, Paul S, Keshavan MS, Nimgaonkar VL, et al. Brain activation patterns during visual episodic memory processing among first-degree relatives of schizophrenia subjects. Neuroimage. 2012; 63:1154–1161. [PubMed: 22992490]
47. Overall JE, Gorham DR. The Brief Psychiatric Rating Scale: A comprehensive review. J Operat Psychiatry. 1991; 148:472.
48. Andreasen, NC. Scale for the Assessment of the Positive Symptoms (SAPS). Iowa, IA: University of Iowa; 1984.
49. Andreasen, NC. Scale for the Assessment of Negative Symptoms (SANS). Iowa City, Iowa: University of Iowa; 1984.
50. Wu, H., Goradia, DD., Stanley, JA. The International Society of Magnetic Resonance in Medicine. Milan, Italy: 2014. A fully automated and robust method of extracting CSI voxels from precise anatomical locations: An application ot a longitudinal ^{31}P MRS study.
51. Jenkinson M, Beckmann CF, Behrens TEJ, Woolrich MW, Smith SM. FSL. NeuroImage. 2012; 62:782–790. [PubMed: 21979382]
52. Dale A, Fischl B, Sereno M. Cortical surface-based analysis. I. Segmentation and surface reconstruction. Neuroimage. 1999; 9:179–194. [PubMed: 9931268]
53. Fischl B, Dale A. Measuring the thickness of the human cerebral cortex from magnetic resonance images. Proceedings of the National Academy of Sciences of the United States of America. 2000; 97:11050–11055. [PubMed: 10984517]
54. Pettegrew JW, Keshavan MS, Panchalingam K, Strychor S, Kaplan DB, Tretta MG, et al. Alterations in brain high-energy phosphate and membrane phospholipid metabolism in first-episode, drug-naive schizophrenics. A pilot study of the dorsal prefrontal cortex by in vivo phosphorus 31 nuclear magnetic resonance spectroscopy. Arch Gen Psychiatry. 1991; 48:563–568. [PubMed: 1898445]
55. Selemon LD, Goldman-Rakic PS. The reduced neuropil hypothesis: a circuit based model of schizophrenia. Biol Psychiatry. 1999; 45:17–25. [PubMed: 9894571]
56. Glantz LA, Lewis DA. Decreased dendritic spine density on prefrontal cortical pyramidal neurons in schizophrenia. Arch Gen Psychiatry. 2000; 57:65–73. [PubMed: 10632234]
57. Glantz LA, Lewis DA. Dendritic spine density in schizophrenia and depression. Arch Gen Psychiatry. 2001; 58:203.
58. Jayakumar PN, Gangadhar BN, Subbakrishna DK, Janakiramaiah N, Srinivas JS, Keshavan MS. Membrane phospholipid abnormalities of basal ganglia in never-treated schizophrenia: a 31P magnetic resonance spectroscopy study. Biological Psychiatry. 2003; 54:491–494. [PubMed: 12915294]
59. Deicken RF, Calabrese G, Merrin EL, Meyerhoff DJ, Dillon WP, Weiner MW, et al. 31phosphorus magnetic resonance spectroscopy of the frontal and parietal lobes in chronic schizophrenia. Biol Psychiatry. 1994; 36:503–510. [PubMed: 7827212]
60. Fukuzako H, Fukuzako T, Takeuchi K, Ohbo Y, Ueyama K, Takigawa M, et al. Phosphorus magnetic resonance spectroscopy in schizophrenia: correlation between membrane phospholipid metabolism in the temporal lobe and positive symptoms. Prog Neuropsychopharmacol Biol Psychiatry. 1996; 20:629–640. [PubMed: 8843487]
61. Kato T, Shioiri T, Murashita J, Hamakawa H, Inubushi T, Takahashi S. Lateralized abnormality of high-energy phosphate and bilateral reduction of phosphomonoester measured by phosphorus-31 magnetic resonance spectroscopy of the frontal lobes in schizophrenia. Psychiatry Res. 1995; 61:151–160. [PubMed: 8545499]

62. Jensen JE, Al-Semaan YM, Williamson PC, Neufeld RW, Menon RS, Schaeffer B, et al. Region-specific changes in phospholipid metabolism in chronic, medicated schizophrenia: (31)P-MRS study at 4.0 Tesla. Br J Psychiatry. 2002; 180:39–44. [PubMed: 11772850]
63. Smesny S, Langbein K, Rzanny R, Gussew A, Burmeister HP, Reichenbach JR, et al. Antipsychotic drug effects on left prefrontal phospholipid metabolism: a follow-up 31P-2D–CSI study of haloperidol and risperidone in acutely ill chronic schizophrenia patients. Schizophr Res. 2012; 138:164–170. [PubMed: 22516552]
64. Volz HP, Rossger G, Riehemann S, Hubner G, Maurer I, Wenda B, et al. Increase of phosphodiesters during neuroleptic treatment of schizophrenics: a longitudinal 31P–magnetic resonance spectroscopic study. Biol Psychiatry. 1999; 45:1221–1225. [PubMed: 10331116]
65. Jayakumar PN, Gangadhar BN, Venkatasubramanian G, Desai S, Velayudhan L, Subbakrishna D, et al. High energy phosphate abnormalities normalize after antipsychotic treatment in schizophrenia: a longitudinal 31P MRS study of basal ganglia. Psychiatry Res. 2010; 181:237–240. [PubMed: 20153149]
66. Volz HP, Rzanny R, Rossger G, Hubner G, Kreitschmann-Andermahr I, Kaiser WA, et al. 31Phosphorus magnetic resonance spectroscopy of the dorsolateral prefrontal region in schizophrenics--a study including 50 patients and 36 controls. Biol Psychiatry. 1998; 44:399–404. [PubMed: 9777168]
67. Palay, SL., Chan-Palay, V. Cellular Biology of Neurons. Kandel, ER., editor. Bethesda, MD: American Physiological Society; 1977. p. 5-37.
68. Anthes DL, LeBoutillier JC, Petit TL. Structure and plasticity of newly formed adult synapses: a morphometric study in the rat hippocampus. Brain Res. 1993; 626:50–62. [PubMed: 8281453]
69. Podo F. Tumour phospholipid metabolism. NMR Biomed. 1999; 12:413–439. [PubMed: 10654290]
70. Pettegrew JW, Panchalingam K, Withers G, McKeag D, Strychor S. Changes in brain energy and phospholipid metabolism during development and aging in the Fischer 344 rat. J Neuropathol Exp Neurol. 1990; 49:237–249. [PubMed: 2335783]
71. Stanley JA, Khatib D, Dick RM, McGarragle OA, MacMaster FP, Robin AL, et al. Evidence of Neuronal Growth Spurts During Development in Healthy Children and Adolescents Using A Multi-voxel In Vivo ^{31}P Spectroscopy at 4 Tesla. International Society of Magnetic Resonance in Medicine Stockholm. 2010
72. Burri R, Lazeyras F, Aue WP, Straehl P, Bigler P, Althaus U, et al. Correlation between 31P NMR phosphomonoester and biochemically determined phosphorylethanolamine and phosphatidylethanolamine during development of the rat brain. Dev Neurosci. 1988; 10:213–221. [PubMed: 3224561]
73. Eriksson SH, Free SL, Thom M, Symms MR, Martinian L, Duncan JS, et al. Quantitative grey matter histological measures do not correlate with grey matter probability values from in vivo MRI in the temporal lobe. J Neurosci Methods. 2009; 181:111–118. [PubMed: 19433106]
74. Lockwood-Estrin G, Thom M, Focke NK, Symms MR, Martinian L, Sisodiya SM, et al. Correlating 3T MRI and histopathology in patients undergoing epilepsy surgery. J Neurosci Methods. 2012; 205:182–189. [PubMed: 22227441]
75. Gilbert AR, Rosenberg DR, Harenski K, Spencer S, Sweeney JA, Keshavan MS. Thalamic volumes in patients with first-episode schizophrenia. Am J Psychiatry. 2001; 158:618–624. [PubMed: 11282698]
76. Rao NP, Kalmady S, Arasappa R, Venkatasubramanian G. Clinical correlates of thalamus volume deficits in anti-psychotic-naive schizophrenia patients: A 3-Tesla MRI study. Indian journal of psychiatry. 2010; 52:229–235. [PubMed: 21180407]
77. van Erp TG, Hibar DP, Rasmussen JM, Glahn DC, Pearlson GD, Andreassen OA, et al. Subcortical brain volume abnormalities in 2028 individuals with schizophrenia and 2540 healthy controls via the ENIGMA consortium. Mol Psychiatry. 2015
78. Knochel C, Stablein M, Prvulovic D, Ghinea D, Wenzler S, Pantel J, et al. Shared and distinct gray matter abnormalities in schizophrenia, schizophrenia relatives and bipolar disorder in association with cognitive impairment. Schizophr Res. 2016

79. Deicken RF, Merrin EL, Floyd TC, Weiner MW. Correlation between left frontal phospholipids and Wisconsin Card Sort Test performance in schizophrenia. Schizophr Res. 1995; 14:177–181. [PubMed: 7710998]
80. Volz HP, Hubner G, Rzanny R, Rossger G, Preussler B, Eichhorn M, et al. High-energy phosphates in the frontal lobe correlate with Wisconsin Card Sort Test performance in controls, not in schizophrenics: a 31phosphorus magnetic resonance spectroscopic and neuropsychological investigation. Schizophr Res. 1998; 31:37–47. [PubMed: 9633835]
81. Meyer U, Feldon J, Yee BK. A review of the fetal brain cytokine imbalance hypothesis of schizophrenia. Schizophr Bull. 2009; 35:959–972. [PubMed: 18408229]
82. Gruol DL. IL-6 regulation of synaptic function in the CNS. Neuropharmacology. 2015; 96:42–54. [PubMed: 25445486]
83. Brucato N, Guadalupe T, Franke B, Fisher SE, Francks C. A schizophrenia-associated HLA locus affects thalamus volume and asymmetry. Brain Behav Immun. 2015; 46:311–318. [PubMed: 25728236]
84. Watanabe D, Yoshimura R, Khalil M, Yoshida K, Kishimoto T, Taga T, et al. Characteristic localization of gp130 (the signal-transducing receptor component used in common for IL-6/IL-11/CNTF/LIF/OSM) in the rat brain. Eur J Neurosci. 1996; 8:1630–1640. [PubMed: 8921254]
85. Gardoni F, Boraso M, Zianni E, Corsini E, Galli C, Cattabeni F, et al. Distribution of interleukin-1 receptor complex at the synaptic membrane driven by interleukin-1beta and NMDA stimulation. Journal of Neuroinflammation. 2011; 8:14. [PubMed: 21314939]
86. Coughlan CM, McManus CM, Sharron M, Gao Z, Murphy D, Jaffer S, et al. Expression of multiple functional chemokine receptors and monocyte chemoattractant protein-1 in human neurons. Neuroscience. 2000; 97:591–600. [PubMed: 10828541]
87. Adler MW, Rogers TJ. Are chemokines the third major system in the brain? J Leukoc Biol. 2005; 78:1204–1209. [PubMed: 16204637]
88. Kitagami T, Yamada K, Miura H, Hashimoto R, Nabeshima T, Ohta T. Mechanism of systemically injected interferon-alpha impeding monoamine biosynthesis in rats: role of nitric oxide as a signal crossing the blood-brain barrier. Brain Res. 2003; 978:104–114. [PubMed: 12834904]
89. Volterra A, Meldolesi J. Astrocytes, from brain glue to communication elements: the revolution continues. Nat Rev Neurosci. 2005; 6:626–640. [PubMed: 16025096]
90. Dunn AJ, Wang J. Cytokine effects on CNS biogenic amines. Neuroimmunomodulation. 1995; 2:319–328. [PubMed: 8840334]
91. Besedovsky H, del Rey A, Sorkin E, Da Prada M, Burri R, Honegger C. The immune response evokes changes in brain noradrenergic neurons. Science. 1983; 221:564–566. [PubMed: 6867729]
92. Levite M. Neurotransmitters activate T-cells and elicit crucial functions via neurotransmitter receptors. Current opinion in pharmacology. 2008; 8:460–471. [PubMed: 18579442]
93. Sarkar C, Basu B, Chakroborty D, Dasgupta PS, Basu S. The immunoregulatory role of dopamine: an update. Brain Behav Immun. 2010; 24:525–528. [PubMed: 19896530]
94. Besser MJ, Ganor Y, Levite M. Dopamine by itself activates either D2, D3 or D1/D5 dopaminergic receptors in normal human T-cells and triggers the selective secretion of either IL-10, TNFalpha or both. J Neuroimmunol. 2005; 169:161–171. [PubMed: 16150496]
95. Erickson MA, Dohi K, Banks WA. Neuroinflammation: a common pathway in CNS diseases as mediated at the blood-brain barrier. Neuroimmunomodulation. 2012; 19:121–130. [PubMed: 22248728]
96. Threlkeld SW, Lynch JL, Lynch KM, Sadowska GB, Banks WA, Stonestreet BS. Ovine proinflammatory cytokines cross the murine blood-brain barrier by a common saturable transport mechanism. Neuroimmunomodulation. 2010; 17:405–410. [PubMed: 20516722]
97. Terreni L, De Simoni MG. Role of the brain in interleukin-6 modulation. Neuroimmunomodulation. 1998; 5:214–219. [PubMed: 9730688]
98. Silverman HA, Dancho M, Regnier-Golanov A, Nasim M, Ochani M, Olofsson PS, et al. Brain region-specific alterations in the gene expression of cytokines, immune cell markers and cholinergic system components during peripheral endotoxin-induced inflammation. Mol Med. 2014; 20:601–611.

99. Avdievich NI. Transceiver-Phased Arrays for Human Brain Studies at 7 T. Applied magnetic resonance. 2011; 41:483–506. [PubMed: 23516332]

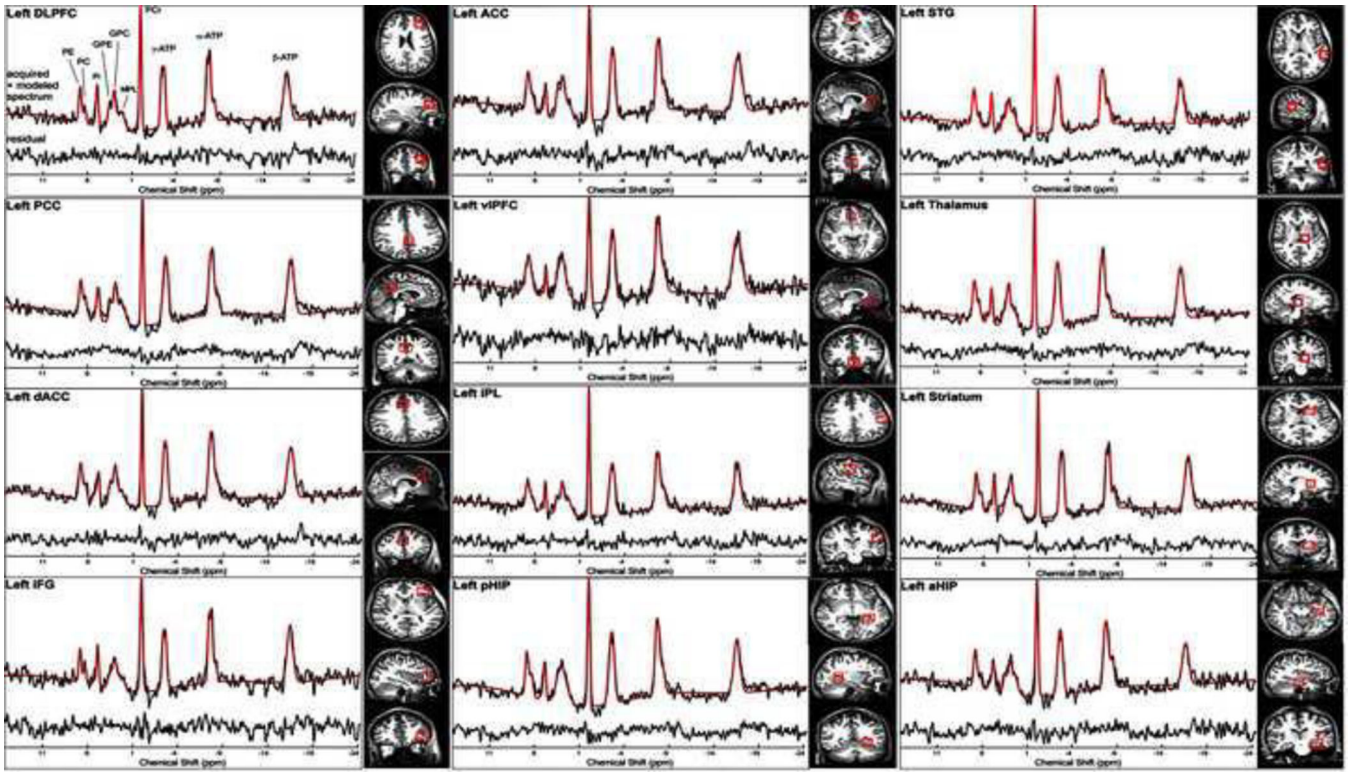

Fig 1.

Voxel placements and representative spectra from each voxel. Only the left sided voxels placements and spectra are shown. Quality of the spectra were high with no significant differences in signal-to-noise (SNR) of PCr between schizophrenia patients and controls. In addition, the Cramer Rao Lower Bound values for both the PC+PE and GPC+GPE were not significantly different between the groups. Legend: DLPFC: Dorsolateral prefrontal cortex; PCC: Posterior Cingulate Cortex; dACC: Dorsal Anterior Cingulate Cortex; IFG: Inferior Frontal Gyrus or Cortex; ACC: Anterior Cingulate Cortex; vPFC: Ventral Prefrontal Cortex; IPL: Inferior Parietal Lobule; pHIP: Dorsal Hippocampus; STG: Superior Temporal Gyrus or Cortex; aHIP: Ventral Hippocampus

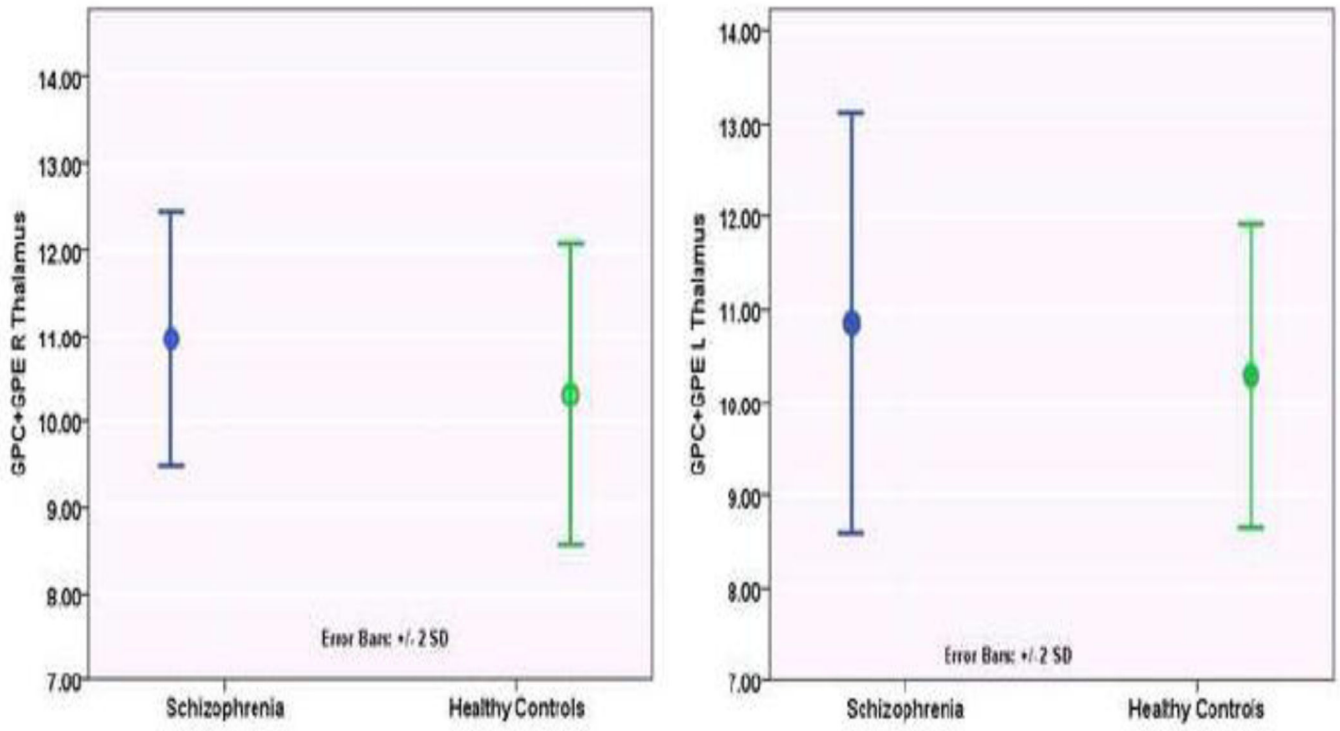

Fig 2.

Comparison of MPL catabolites (GPC+GPE) in the thalamus between schizophrenia patients and healthy controls. In addition, the dorsolateral prefrontal cortex, ventral hippocampus, inferior frontal cortex, inferior parietal lobule and superior temporal gyrus also showed diagnosis main effect (Overall model, $F(24, 614)=8.19$, $p<0.001$). While GPC +GPE levels were elevated in bilateral thalamus and right ventral hippocampus it was reduced in the right dorsolateral prefrontal cortex, right inferior frontal cortex, and bilateral inferior frontal lobule, superior temporal gyrus in schizophrenia compared to controls. See Table 2 for percentage differences at these voxels-of-interest between the groups.

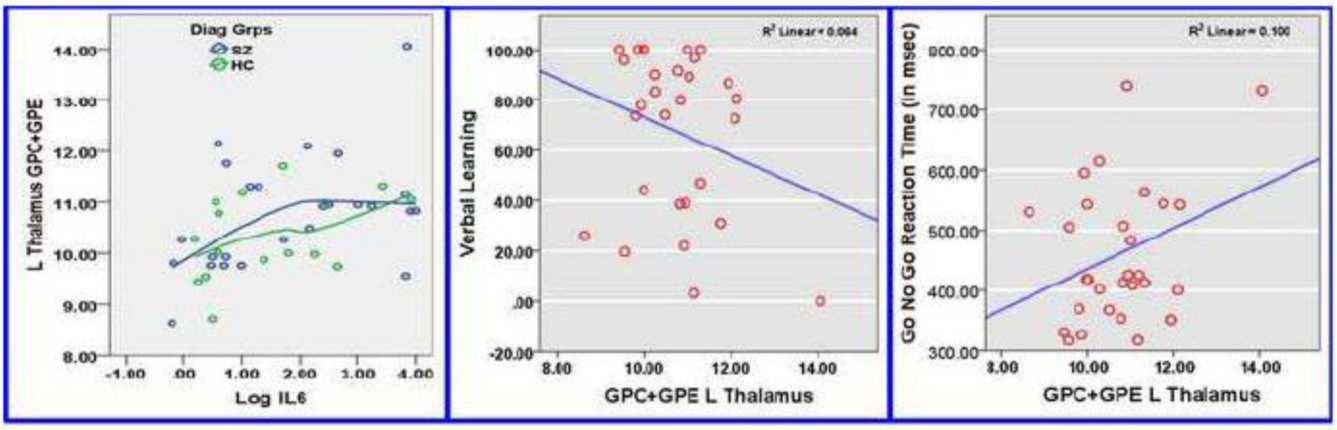

Fig 3.

Relationship of GPC+GPE (MPL catabolites) with IL-6 levels (left), verbal learning (middle) and sustained attention (right). *Left*: Correlation of GPC+GPE in the thalamus with IL-6 levels is shown with LOWESS regression plot using triweight approach to weigh each k-nearest neighbor. *Middle*: Negative correlation of GPC+GPE in the left thalamus with vernal learning performance. After correction for multiple testing, this correlation remained a trend. *Right*: Positive correlation of GPC+GPE in the left thalamus with Go-No-Go response time. Increasing IL-6 levels were related to prolonged processing time.

Table 1

Demographic and Clinical variables of early course schizophrenia and healthy control subjects

	Schizophrenia	Healthy Controls	Statistic	Significance
Age	25.15±8.03	25.24±6.25	t=0.04	0.97
Sex Male Female	18 10	5 16	$\chi^2 = 7.89$	0.009
SES Mother Father	31.56±14.67 35.73±15.70	41.28±14.55 46.42±12.09	t=1.90 t=1.90	0.07 0.06
IL-6	24.99±8.49	24.52±4.60	t=0.20	0.84
CRP	24.16±7.36	25.94±6.16	t=0.64	0.53
WLMPTT	56.65±30.80	91.88±15.04	F(1,34)=18.14	<0.001
WCST Percent Perseverative Error	19.42±9.71	12.51±10.27	F(1,34)=4.18	0.049
Go No Go Response Time	488.03±128.58	396.42±61.78	F(1,34)=7.08	0.012
SANS Total	11.00±3.46	--	--	--
SAPS Total	2.94±2.65	--	--	--
BPRS Negative Symptoms	7.89±3.71	--	--	--
BPRS Positive Symptoms	8.61±3.65			
Antipsychotic treatment Dose Mean number of days of treatment	317.53±270.20mg * 488.93±320.71			
Other psychotropic medications[1,2] Lithium (n=3 patients) Oxcarbazepine (n=1 patients) Citalopram (n=1 patient) Fluoxetine (n= 2 patients)	900–1500 mg/day (189–883 days) 600 mg/day for 572 days 20 mg for 252 days 20 mg (194 and 957 days)			

* Chlorpromazine equivalents per day. One patient received clozapine suggesting that this patient might have failed at least two other antipsychotics. We were unable to obtain data on other two antipsychotics received by this patient. Other patients were on olanzapine, risperidone, ziprasidone, quetiapine and aripiprazole. One patient was cross-tapered from risperidone to aripiprazole and then to quetiapine.

1 Precise end dates were not available for all.

2 One patient received various medications that included fluoxetine (already shown in the table), chlordiazepoxide, clonazepam, lorazepam, and benztropine at various points in time; benzodiazepines given as needed (prn). At the time of consenting and imaging, this subject was on venlafaxine and 150 mg per day and clonazepam 0.5 mg.

Table 2

Voxels of interest that showed significance differences in MPL catabolites between persons with schizophrenia and healthy controls

Metabolite	Region	Statistics				Schizophrenia		Healthy Controls			
		B	95% CI of B	t	Corrected p*	Mean	SD	Mean	SD	Percentage difference	Effect size (Cohen's *d*)
GPC+GPE	L. Thalamus	0.39	(0.02 – 0.76)	2.07	0.039	10.86	1.13	10.21	0.76	6.37	0.68
	R. Thalamus	0.49	(0.09 – 0.90)	2.39	0.017	10.96	0.73	10.38	0.85	5.59	0.73
	R. Ventral Hippocampus	0.62	(0.08– 1.15)	2.26	0.024	10.28	1.12	10.07	1.46	2.09	0.16
	R. Dorsolateral Prefrontal Cortex	−1.01	(−1.45– −0.57)	−4.5	<0.001	8.55	1.15	9.78	1.94	−12.58	−0.77
	L. Inferior Parietal Lobule	−1.06	(−1.58– −0.55)	−4.09	<0.001	8.11	1.61	9.88	2.44	−17.91	−0.86
	R. Inferior Parietal Lobule	−1.39	(−1.98– −0.80)	−4.65	<0.001	8.30	1.42	8.98	2.50	−7.57	−0.33
	R. Inferior Frontal Cortex	−1.91	(−2.46 – −1.37)	−6.92	<0.001	7.81	1.76	8.09	1.34	−3.46	−0.18
	L. Superior Temporal Gyrus	−1.09	(−1.53– −0.66)	4.91	<0.001	8.48	1.59	9.59	1.70	−11.57	−0.67
	R. Superior Temporal Gyrus	−1.09	(−1.68– −0.50)	−3.64	<0.001	8.90	1.80	9.15	2.15	−2.73	−0.13
PC+PE	R. Ventral Hippocampus	1.16	(0.76 – 1.57)	5.6	<0.001	12.51	1.88	11.14	1.29	12.30	0.85
	R. Dorsal Hippocampus	1.08	(0.79 – 1.36)	7.4	<0.001	12.04	0.74	11.52	0.81	4.51	0.67
	L. Ventral Hippocampus	1.01	(0.57 – 1.45)	4.49	<0.001	11.94	1.48	11.46	1.30	4.19	0.34
	L. Dorsal Hippocampus	0.84	(0.46 – 1.22)	4.37	<0.001	11.91	1.46	11.41	0.86	4.38	0.42

Metabolite	Region	Statistics				Schizophrenia		Healthy Controls			
		B	95% CI of B	t	Corrected p*	Mean	SD	Mean	SD	Percentage difference	Effect size (Cohen's *d*)
	L. Anterior Cingulate Cortex	0.35	(0.03–0.67)	2.12	0.035	11.55	1.51	10.90	1.08	5.96	0.50
	L. Inferior Frontal Cortex	−0.62	(−1.15–−0.09)	−2.3	0.023	10.30	1.83	15.57	22.54	−33.85	−0.33
	R. Inferior Frontal Cortex	−0.81	(−1.26–−0.036)	−3.56	<0.001	9.61	1.39	10.04	1.99	−4.28	−0.25
	L. Inferior Parietal Lobule	−0.43	(−0.84–−0.01)	−2.01	0.045	9.83	1.28	10.68	1.75	−7.96	−0.55